Fuel 290 (2021) 120054

Contents lists available at ScienceDirect

Fuel

journal homepage: www.elsevier.com/locate/fuel

Full Length Article

Connecting gasification with syngas fermentation: Comparison of the performance of lignin and beech wood

E.T. Liakakou [a,1,*], A. Infantes [b,1], A. Neumann [b], B.J. Vreugdenhil [a]

[a] TNO Energy Transition, Biobased and Circular Technologies, Westerduinweg 3, Petten 1755 LE, Netherlands
[b] KIT, Institute of Process Engineering in Life Science 2: Technical Biology, Karlsruhe Institute of Technology, Fritz-Haber-Weg 4, 76131 Karlsruhe, Germany

ARTICLE INFO

Keywords:
Lignin gasification
Indirect gasification
Biorefinery
Syngas fermentation
Biofuels
Clostridium ljungdahlii

ABSTRACT

The integration of gasification with syngas fermentation is still in an early stage of development, where many questions exist concerning the syngas quality required. The challenge is to define the gasification conditions that will provide a H_2:CO:CO_2 ratio suitable for syngas fermentation, as well as to identify and remove the compounds that can inhibit the performance of the microorganisms. The right balance between the gasification conditions and a line up with minimal gas cleaning needs to be assessed to improve the economic feasibility of the process. In this work a first attempt to combine the two processes is presented, with the aim to provide an insight of the indirect gasification, the gas cleaning applied, the effect of the main impurities and the performance of syngas fermentation. A lignin rich feedstock was gasified with steam in an indirect gasifier, at TNO (Netherlands Organization for Applied Scientific Research). The gas, after removal of some components that could hinder the performance of the fermentation (tar compounds, BTX, unsaturated hydrocarbons and sulphur compounds), consisted of CO, H_2, CO_2, CH_4, C_2H_6 and traces of other hydrocarbons. The influence of the obtained syngas quality and composition was evaluated in the fermentation process using *Clostridium ljungdahlii*, at KIT (Karlsruhe Institute of Technology). For comparison, product gas from beech wood gasification was also evaluated in the fermentation process under the same conditions.

1. Introduction

The development of lignin derived energy products is one way to increase the value of biorefinery residues, which is the scope of the EU project AMBITION [1]. Second generation biorefineries for the production of bioethanol use pre-treatment technologies where lignin ends up in a residue together with unconverted fibers, feedstock minerals, and process chemicals. This type of residue is usually exploited in a rather low-added-value application, such as combined heat and power generation. Another alternative to utilize the lignin-rich biorefinery residues is to produce a gas, via gasification, [2–5] that can be converted to higher-added-value products, such as liquid fuels and chemicals.

In a previous study, [6] different gasification technologies were compared for the valorization of lignin-rich residues, obtained from the production of second generation bioethanol. The indirect or allothermal gasification allows high feedstock conversion and also better control and process optimization. The combustion products (flue gas) and gasification products (product gas or synthesis gas) are not mixed. This means that the product gas is not diluted with N_2 coming from the air used for combustion, and thus, is suitable for synthesis applications after proper cleaning and upgrading without the need for an expensive air separation unit. Furthermore, indirect gasification produces a high value gas which contains compounds such as CH_4, C_2-C_4 gases (including ethylene and acetylene), benzene, toluene and xylene (BTX), and tar. The separation of the most valuable components of the product gas is an efficient way to maximize the value from the feedstock via co-production schemes [7].

The product gas, after appropriate cleaning to remove impurities that can reduce its fermentability, can be used in a biological process to produce biofuels. Syngas fermentation has been called a “hybrid thermochemical/biochemical process” because of the nature of the joint process. Acetogenic bacteria can be used as biocatalysts for the microbial conversion of syngas into short-chain organic acids and alcohols, such as ethanol and acetate [8–10]. The ability of these microorganisms to withstand some of the impurities contained in the syngas and their flexibility to use different mixtures of CO and/or CO_2 and H_2 makes them an attractive alternative to the chemical catalytic processes.

* Corresponding author.
E-mail address: eleni.liakakou@tno.nl (E.T. Liakakou).
[1] Liakakou and Infantes share first authorship.

https://doi.org/10.1016/j.fuel.2020.120054
Received 24 June 2020; Received in revised form 16 November 2020; Accepted 20 December 2020
Available online 31 December 2020

Moreover, the process conditions for microbial conversion are milder with respect to pressure and temperature compared to chemical processes, resulting in reduced operating costs [10–12]. However, the integration of gasification with syngas fermentation is still in an early stage of development, where many questions exist concerning the syngas quality needed in the fermentation process.

For the integration of lignin-rich residues gasification with syngas fermentation, it is of utmost importance to understand how the feedstock properties impact the product gas composition and which compounds present in the final syngas have an inhibitory effect on the microorganisms. These two factors have a strong influence in the fermentation outcome [13,14]. Removing the impurities from the syngas has an important impact on the process costs [15]. Thus, the right balance has to be found, in order to prevent excessive, unnecessary cleaning steps. Acetogenic microorganisms performing syngas fermentation have proved to be resistant towards higher levels of impurities compared to traditional catalysts [10]. Besides, microorganisms can be adapted to the presence of certain impurities [8]. By investigating which compounds act as inert for the fermentation, the syngas production and cleaning strategy can be optimized to improve the fermentation outcome, hence reducing the overall costs.

According to literature, [13,16–18] the main requirement for syngas for fermentation is low contents of contaminants like tar, acetylene, ethylene and benzene, as they inhibit enzymes responsible for the initial harvesting of carbon and energy from syngas in acetogenic organisms. Most organisms grow better by using CO as the only energy and carbon source or with CO as the carbon source and CO/H_2 as the energy source [18]. As a result, the H_2 to CO ratio can be low, i.e. additional reforming steps and water–gas shift reaction after gasification are not needed. Most acetogens are also able to grow and produce ethanol from CO_2 and H_2, providing direct CO_2 sequestration into products [19]. However, many of these characteristics, such as the tolerance to sulphur, will depend on the particular type of organism used [9].

Syngas fermentation has been chosen as an attractive conversion route by several companies for pilot-, demo- and near commercial-scale cellulosic ethanol production [9]. However, two of the three companies that operate scaled up gas fermentation facilities suspended their operation by 2016 [20]. Coskata was addressing ethanol production in a demo- unit, first using syngas from biomass gasification and later from methane reforming but went out of business in 2015 [21]. INEOS New Planet BioEnergy developed a syngas-to ethanol process but stopped the operations by 2016 due to the high levels of hydrogen cyanide in syngas [22]. LanzaTech is successfully deploying two commercial ethanol-producing facilities using off-gases and is also moving towards the biomass sector with two commercial-scale projects under development, using syngas produced from agricultural waste and municipal solid waste [23,24].

Despite the recent developments, challenges associated with the scale-up and operation of this novel process, such as low mass transfer efficiency and the presence of inhibitory compounds in syngas still remain. In this work we report a first approach to combine the indirect gasification of lignin-rich residues with syngas fermentation. The important focus point is the gas quality, since the requirements for syngas fermentation are different compared to chemical catalytic processes. Product gas from the lignin-rich feedstock gasification, after appropriate cleaning and conditioning to remove impurities that can reduce the fermentability of the gas (such as tars, BTX, unsaturated hydrocarbons, HCN, HCl, COS and other organic S-compounds), is utilized in the fermentation process using *C. ljungdahlii* for the production of acetate and ethanol. Product gas from beech wood gasification is also used in the fermentation process under the same conditions, in order to compare the two feedstocks.

2. Experimental

2.1. Feedstock properties

The lignin-rich feedstock, which was received from a biorefinery, is originating from wheat straw, after steam explosion and enzymatic hydrolysis. Following this pre-processing, it was filter pressed and therefore consisted of big dense particles. The pretreatment of this feedstock (from now on referring as lignin) was described in detail elsewhere [6]. Beech wood was received in chips and no pretreatment was required before feeding it to the gasifier. The feedstocks, as used in the indirect gasification tests, are shown in Fig. 1.

Table 1 shows the most relevant thermochemical properties of the feedstocks for the gasification process and for the quality of the gas going to the fermentation process. A detailed list of the thermochemical properties of the lignin can be found elsewhere [6]. As can be seen, the amount of volatile matter is lower for lignin compared to beech wood, which affects the hydrodynamics in the gasifier. The most noticeable aspect is the high ash content of lignin (14 wt%), consisting mainly of silica (5.4 wt% of the feedstock) with minor amounts of calcium (0.5 wt %) and potassium (0.3 wt%) [6]. This could lead to agglomeration and corrosion issues at high temperatures (above 900 °C) due to alkali-silicate melt phase formation and build-up on the bed material [25,26]. For this reason, it was decided to perform the lignin gasification test at lower temperature than beech wood (<800 °C). Furthermore, the sulphur and nitrogen content of lignin is relatively high compared to wood, due to the higher content of the corresponding compounds in the original feedstock [27]. This could lead to high S- and N- compounds in the product gas (such as H_2S, COS, NH_3, etc.). Depending on the microorganism's resistance to these compounds, a suitable gas conditioning method needs to be applied for their removal.

2.2. Description of the experimental set-ups and product analysis

2.2.1. MILENA indirect gasification

The MILENA gasifier was developed for the gasification of biomass, and the process is based on indirect or allothermal gasification [28]. In one reactor the fuel is gasified or pyrolyzed using hot bed material. There, because of the relatively low temperature (typically 850 °C) of the pyrolysis process, the conversion of the fuel is limited. The remaining char is combusted in a separate reactor. The heat from the combustion is used to heat the circulating bed material. In the typical wooden biomass configuration the gasification takes place in the riser reactor where the residence time of the fuel is relatively short, but sufficient for the reactive feedstock.

After the previous test in riser gasification mode with the same lignin, [6] the results showed that the fuel conversion was insufficient, so the MILENA configuration was converted to operate inversely. A schematic layout and a picture of the so-called i-MILENA concept is given in Fig. 2. The feedstock is added to the bubbling fluidized bed zone (BFB) via a feeding screw. The BFB acts as steam gasification reactor, thus allowing longer residence times (in the order of 10–20 min) of the fuel particles compared to the MILENA concept in order to cope with less reactive (low volatile, high ash) feedstock. Furthermore, the process conditions in the steam blown bubbling fluidized bed gasifier are optimum for primary tar reduction, due to the better contact between the (catalytic) bed material and the feedstock than in the riser and also because an excess of steam is available for tar reforming. The heat required for the endothermic steam gasification reactions is created by combustion of the remaining coke in the riser zone using air. Additional heat is provided to the BFB reactor by tracing, due to the restricted size of the riser combustor. Hot bed material ejected from the top of the riser is separated from flue gas in the settling chamber and recirculated through the downcomer to the BFB gasification zone. Producer gas leaves the gasifier on the side and exits the system via a cyclone.

Fresh Austrian olivine, a mineral based on an iron-magnesium

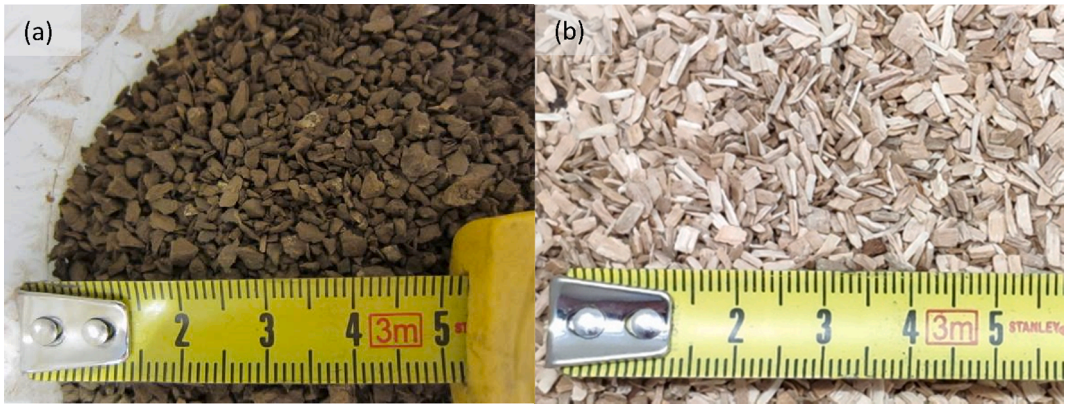

Fig. 1. Lignin (a) and beech wood (b) as used in the gasification tests.

Table 1
Thermochemical properties of lignin and beech wood feedstocks.

	Lignin	Beech wood	Norm used
Ultimate analysis (wt.%, dry basis)			
C	47.2	48.8	NEN-EN-ISO 16948
H	5.6	6.0	NEN-EN-ISO 16948
O	33.0	44.5	No standard present
N	1.3	0.14	NEN-EN-ISO 16948
S	0.18	0.02	NEN-EN-ISO 16994
Cl	0.020	0.005	NEN-EN-ISO 16994
Proximate analysis (wt.%, dry basis)			
Ash 550 °C	14.0	1.0	NEN-EN-ISO 18122
Volatile matter	64.6	83.0	NEN-EN-ISO 18123

orthosilicate structure ($FeMgSiO_4$), was employed as the bed material. CO_2 was used to flush the fuel feeding screw and to carry the steam in the riser combustor reactor. The detailed operating conditions are shown in Table 2. The gasification temperature was approximately 760 °C for lignin and 860 °C for beech wood and steam fluidization was conducted at 2.2 kg/h and 1.0 kg/h, respectively. Higher steam flow was used for lignin gasification, compared to beech wood, in order to reach the minimum fluidization velocity in the BFB. Additional nitrogen was also used periodically in this lab-scale test, to compensate for reduced gas flow in the BFB, due to difficulties feeding sufficient feedstock. The gasification system was operated at atmospheric pressure. Tracer gases, such as Ne and Ar, were added downstream of the gasifier for flow determination.

2.2.2. *Product gas cleaning*

The layout of the gasification and gas cleaning process is shown in Fig. 3, indicating the product gas sampling positions. A slipstream of dry produced gas from the MILENA gasifier was directed at approximately 1000 NL/h to the system downstream and the rest was sent to the afterburner. The OLGA tar removal unit, a staged oil-based scrubbing system, almost completely separated the gas from tar compounds heavier than BTX. The separated tar compounds can be circulated to the combustor reactor of the gasifier, covering the energy needs of the process. More details on the OLGA tar removal unit can be found elsewhere [7].

Neon gas was injected at 0.01 NL/min as tracer gas upstream OLGA to be able to check molar balances over the downstream system. Since lignin has a high sulphur content (shown in Table 1), the product gas contained significant amount of H_2S that was captured by an Activated Carbon (AC) bed, containing a commercial AC adsorbent, operating at

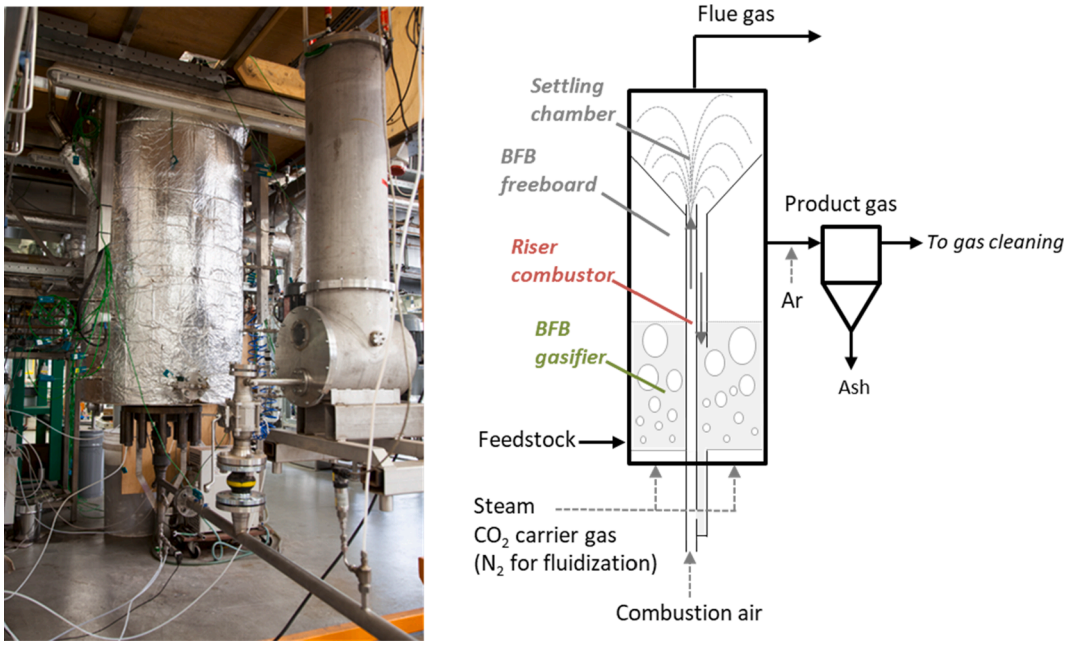

Fig. 2. Picture and schematic layout of the 25 kW i-MILENA gasifier as used for lignin and beech wood gasification.

Table 2
Gasification conditions used in i-MILENA indirect gasifier.

Gasification conditions	Lignin	Beech wood
T in BFB gasifier (°C)	760	860
Fuel, dry (kg/h)	3.4	3.6
Fuel moisture content (wt.%)	3.3	9.0
Steam (kg/h)	2.2	1.0
Carrier gas CO_2 (NL/min)	2.3	2.2
Tracer gas Ne upstream OLGA (NL/min)	0.01	0.01
Tracer gas Ar downstream MILENA (NL/min)	1	1
Combustion air in riser (NL/min)	100	100

Values are at Normal conditions at temperature of 0 °C (273.15 K) and absolute pressure of 1 atm (1.01325×10^5 Pa).

80 °C. A fixed bed reactor was used, with external trace heating and a series of thermocouples to measure the axial temperature profile over the reactor.

Subsequently, most of the water in the product gas was removed by a condenser operating at 10 °C to reduce the gas moisture content to around 1%. The condenser (shown in Fig. 3) does not only remove water from product gas, but can have a large effect on water soluble compounds, especially HCl and NH_3 (not measured here). The gas flow varies with time, as the flow resistance over the system changes. Flow resistance varies mainly over the hot gas filter upstream of the OLGA. The BTX scrubber, which was developed by TNO (shown in Fig. 3 and Fig. 4), is a system for the separation of BTX and traces of additional hydrocarbons by using an absorption liquid. It consists of an absorber and a stripper column, which are filled with structured packing. A dedicated oil absorbs selectively BTX in the absorber at 35 °C. The absorption liquid loaded with BTX is subsequently stripped from BTX using steam in the stripper column. The recovery of the high-value bio-BTX compounds can generate additional income and effectively improve the economic benefit of the gasification process [7]. The clean and dry product gas was compressed to about 5 bar by a frequency-regulated compressor. This compressor controls the flow through the units downstream MILENA and thereby the slipstream.

A commercial CoMoO catalyst is used in the hydrodesulphurisation (HDS) reactor in order to convert the organic sulphur compounds (e.g. thiophene) into mainly H_2S and COS, as well as hydrogenate alkenes and alkynes into alkanes (e.g. C_2H_4 and C_2H_2 into C_2H_6). The HDS unit (shown in Fig. 4) consists of a catalytic fixed-bed reactor with three external trace heating zones to compensate for heat loss and thermocouples along the reactor axis. The water gas shift (WGS) reaction can also take place in this reactor. The operating pressure is approximately 5 bar and the trace heating zones are set at 300 °C (top), 370 °C (middle), and 480 °C (bottom). The target flow rate of gas entering the HDS was 11–12 NL/min in order to keep a GHSV (Gas Hourly Space Velocity) of 200–250 h^{-1}.

The produced H_2S (and COS) is removed from the gas downstream in two adsorption beds (shown in Fig. 3 and Fig. 4). Both fixed bed reactors are provided with external trace heating and a series of thermocouples to measure the axial temperature profile over the length of the reactor.

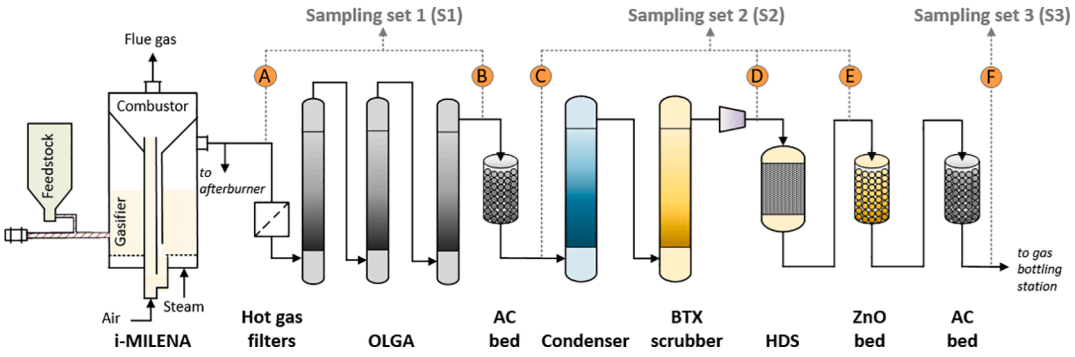

Fig. 3. Experiment layout of the gasification and gas cleaning process, as applied during the gas bottling campaigns at TNO. The product gas sampling positions are also indicated.

Fig. 4. Picture of OLGA (left), BTX scrubber (middle), HDS unit and fixed bed reactors for sulphur removal (right).

The first fixed bed contains a commercial AC adsorbent and operates at room temperature and 5 bar. The second contains a commercial ZnO adsorbent and is kept at a temperature of 250 °C and pressure of 5 bar. Traces of BTX are also captured by the ZnO and AC adsorption beds.

The product gas is cooled to 4 °C to remove any traces of water before it is bottled. The bottles were received by the supplier with N_2 atmosphere (3–4 bar). In order to minimize its concentration in the final bottled syngas, the bottling procedure was as follows: firstly, the N_2 was released from the bottles (down to 0.5–1.2 bar), then, they were filled one time with product gas up to 5 bar, the whole content was flushed down to 0.5–0.9 bar and filled again with product gas up to the maximum system pressure (5 bar). In total, 750L of clean product gas from beech wood and 750L from lignin gasification were bottled and sent to KIT for the fermentation experiments.

2.2.3. Product gas analysis

The product gas was sampled for analysis at 6 different positions, A–F (see Fig. 3), using three different sampling sets. Sampling set 1 (S1) was used for the raw product gas (position A: downstream MILENA gasifier and position B: downstream OLGA), sampling set 2 (S2) was used for the conditioned gas (position C: downstream the AC bed, position D: downstream the condenser and BTX scrubber, position E: downstream the HDS reactor) and sampling set 3 (S3) was used for the clean gas after the ZnO and the final AC guard bed (position F: before gas bottling station).

At every gas analysis sampling position, a slip stream of the product gas was cooled down to 5 °C to remove the condensate (water and tar compounds) from the gas in order to protect each gas analysis set. Online monitoring of product gas (H_2, CO, CO_2, CH_4) and flue gas (O_2, CO_2, CO, CxHy, N_2O, NO, NO_2) was carried out by the three analytical sets. ABB CALDOS 17 Thermal Conductivity Detector was used for H_2, ABB URAS 14 Non Dispersive Infra-Red Analyser (NDIR) for CO, CO_2, CH_4, N_2O, SO_2, ABB MAGNOS 16 Para- Magnetic O_2 sensor for O_2, Ratfisch RS55 Flame Ionisation detector was used for the trace hydrocarbons in the flue gas and ABB LIMAS 11 UV detectors for NO and NO_2. Additionally, the product gas composition was measured online by the three analysis sets using a micro-GC (Varian Micro-GC CP 4900). The product gas was also sampled for offline analysis of the trace hydrocarbons (GC-FID) and sulphur compounds (GC-FPD). Additionally, the SPA method was used for the determination of the content and composition of the tar compounds in the product gas, at positions A and B, following the CEN/TS 15439:2006 procedure.

2.2.4. Syngas fermentation experimental set-up and analytical methods

The microorganism used for the syngas fermentation was *Clostridium ljungdahlii* DSM 13528, because it is one of the most well-characterized strains, used broadly as a model for acetogenic bacteria in fermentation experiments with model syngas. Pre-cultures were grown on fructose in order to obtain higher bacterial biomass concentrations, as well as to avoid any potential pre-adaptation to the syngas. The medium and the cultivation conditions used can be found elsewhere [8]. The fermentations were performed in triplicates which were run simultaneously. These were carried in 3 Minifors bench-top stirred tank reactors, shown in Fig. 5 (Infors-HT, Switzerland), which have a total volume of 2.5 L. The working liquid volume is 1.5 L. The gas for the fermentation was supplied by means of a microsparger, while the gas flow rate was controlled via a mass flow controller (MFC) red-y smart series, from Vögtlin Instruments (Switzerland). The temperature of the fermenter was kept at 37 °C, pH was controlled at 5.9 with 4 M KOH and stirring was regulated at 800 rpm. A detailed description of the fermenter set-up can be found elsewhere [8].

The fermentation experiments were performed using real syngas produced from beech wood and lignin gasification by TNO. Anaerobic conditions were ensured after autoclaving by sparging the fermenters with N_2 for 2 h. Following this, the gas supply was changed to syngas with a flow rate of 50 mL/min for at least 3 h until just before inoculation, when the gas flow rate was adjusted as required. Due to the differing gas composition of all the gases tested, not all parameters could be kept constant simultaneously. The gas flow rate was adapted in each fermentation so that the total amount of carbon (the sum of CO_2 and CO) fed into the fermenter was approximately 0.4 mmol/min. As a result, the amount of H_2 fed to the fermenters differed between the experiments, at 0.2 mmol/min for the beech wood syngas (BWS) and 0.3 mmol/min for the lignin syngas (LS). For the fermentation of the BWS, the gas flow rate was controlled at 18 mL/min and for LS, the flow rate used was 23 mL/min.

Table 3 shows the average composition of the gas flow fed into the fermenter, measured after the reactor reached equilibrium, and under abiotic conditions, i.e. before inoculation. The gas flow fed into the fermenter equals then to that coming out in the off-gas. Despite the fact that the gas bottling took place after cleaning and conditioning as described in the previous chapter, some unidentified impurities might still be present in the syngas.

The fermenters' off-gas was analyzed using a GC-2010 Plus AT gas chromatograph (GC) (Shimadzu, Japan), with a ShinCarbon ST 80/100

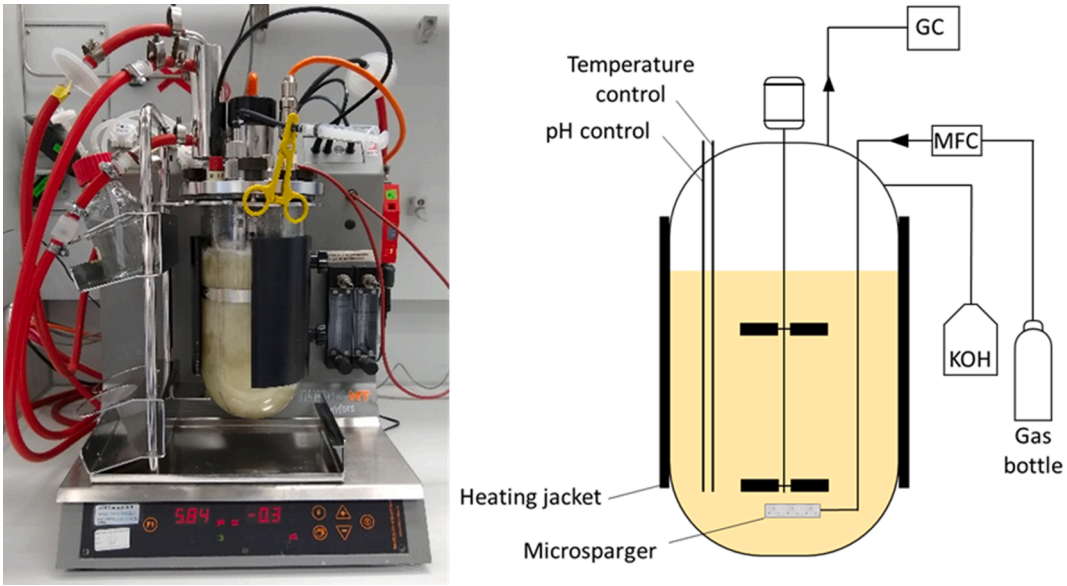

Fig. 5. 2.5 L glass stirred tank reactor used for the syngas fermentation tests. The working volume was 1.5 L.

Table 3
Gas composition and flow rates - values measured with process GC directly before inoculation.

		H_2	CO	CO_2	CH_4	CO + CO_2	H_2/(CO + CO_2)	H_2/CO	Gas flow rate (NmL/min)
Beech wood syngas	Composition (%)	22.7 ± 0.5	28.5 ± 0.2	19.1 ± 0.3	9.9 ± 0.0	47.6	0.5	0.80	18
	Molar flow (mmol/min)	0.18 ± 0.0	0.23 ± 0.0	0.15 ± 0.0	0.08 ± 0.0	0.38			
Lignin syngas	Composition (%)	27.0 ± 0.1	21.3 ± 0.1	18.0 ± 0.2	10.6 ± 0.0	39.3	0.7	1.27	23
	Molar flow (mmol/min)	0.28 ± 0.0	0.22 ± 0.0	0.19 ± 0.0	0.10 ± 0.0	0.41			

Values are at Normal conditions at temperature of 0 °C (273.15 K) and absolute pressure of 1 atm (1.01325×10^5 Pa).

Column (2 m × 0.53 mm ID, Restek, Germany) and a Rtx-1 capillary column (1 μm, 30 m × 0.25 mm ID, Restek, Germany). A thermal conductivity detector with helium as the carrier gas was used. The sampling regime was as follows: four samples of 2 mL were daily taken at 2–3 h intervals, with no sample collection taking place overnight. These were then used for OD (optical density) determination and left-over fructose (from the pre-culture) and products (acetate and ethanol) concentration. The OD (optical density) was measured at 600 nm, and OD and cell dry weight (CDW) correlation was determined as the average of 12 fermentations under comparable conditions (data not shown), with a resulting factor of CDW/OD = 0.3 g/L/OD. The sample collection, treatment, off-line analysis and data processing are described in detail elsewhere [8].

The parameters gas consumption profile, yields, productivity, acetate to ethanol ratio, as well as the percentage of carbon fixed were calculated for the three different, relevant time frames: the complete run (endpoint), up to the point when maximum CO consumption stopped (CO fixation) and during the interval of maximum overall usage. The maximum overall usage interval is calculated from the gas consumption profile and represents the period in which the usage value of the gaseous substrates is above 85% of the maximum achieved during the fermentation. For each fermentation, the sum of the usage of each gas (CO, H_2 and CO_2) is calculated, and the maximum usage is identified. The percentage of carbon fixed ($E_{C,\ total}$), expressed in mol %, is the sum of CO_{used} and $CO_{2\ used}$ per total carbon fed (CO_{fed} plus $CO_{2\ fed}$). If CO_2 is produced, then the sum of CO_{used} and $CO_{2\ used}$ is CO_{fixed}. A detailed explanation of the terms used and the calculations performed can be found elsewhere [29]. Endpoint calculations were done using the values measured with the sample taken immediately before terminating the fermentation. More details regarding the yield calculations (yield per substrate fed ($Y_{P/S,\ fed}$), yield per substrate used ($Y_{P/S,\ used}$), and yield per substrate fixed ($Y_{P/S,\ fixed}$)) and the terminology used can be found elsewhere [29].

3. Results and discussion

3.1. Gasification

3.1.1. Beech wood

The i-MILENA gasifier operated under stable conditions during beech wood gasification for more than six hours. The average temperature in the BFB gasification reactor during the steady operation, given by 3 thermocouples located at the bottom, middle and top part of the bed, is around 860 °C. The average temperature in the riser combustor is also 860 °C.

The average composition of the gas – on dry basis – is reported in Table 4. Graphical representation of the gas components concentration with time at all measured positions, can be found in the supplementary material. At position A (downstream i-MILENA) was 33.4 vol% H_2, 28.0 vol% CO, 23.8 vol% CO_2 and 8.8 vol% CH_4. However, 3.3 vol% of the CO_2 is due to the CO_2 that is used as a carrier gas in the feeding screw and steam generator, as shown in Fig. 2. The H_2/CO ratio was 1.2, which is a typical value for woody biomass gasification [28]. The use of olivine as bed material results in enhanced H_2 production and decreased CO and

Table 4
Gas composition over the sampling positions S1, S2 and S3 during beech wood gasification and gas cleaning.

Gas component	Analysis method	Unit	Position A (Downstream MILENA)	Position B (Downstream OLGA)	Position C (Downstream AC)	Position E (Downstream BTX/HDS)	Position F (Downstream AC/ZnO)
Average sampling period (h)			2–2.5	3–3.5	3–3.3	5–5.8	3–8
CO	Gas monitor	Vol%	28.8	30.4	31.2	32.3	32.3
H_2	Gas monitor	Vol%	32.1	31.9	31.8	28.3	28.5
CO_2	Gas monitor	Vol%	25.2	21.9	22.4	23.2	23.3
CH_4	Gas monitor	Vol%	8.8	9.1	9.2	11.3	11.7
N_2	Gas monitor	Vol%	1.2	1.4	1.3	1.4	1.6
C_2H_2	micro GC	Vol%	0.03	0.14	0.14	<0.001	<0.001
C_2H_4	micro GC	Vol%	1.6	1.7	1.7	<0.001	<0.001
C_2H_6	micro GC	Vol%	0.05	0.06	0.06	2.37	2.49
Benzene	micro GC	ppmV	6022	4684	4746	86	13
Toluene	micro GC	ppmV	211	320	232	<10	<10
Sum C3	GC-FID	ppmV	85	113	103	291	323
Sum C4	GC-FID	ppmV	87	16	185	106	37
Sum C5	GC-FID	ppmV	51	1	83	17	63
Sum C6	GC-FID	ppmV	7	19	18	<1	8
H_2S	S-GC	ppmV	115	89	<0.5	7	<0.5
COS	S-GC	ppmV	4	6	0.8	<0.5	<0.5
Other S-	S-GC	ppmV	3	4	2	<0.5	<0.5
Ne tracer gas	micro GC	ppmV	–	898	935	932	964
Ar tracer gas	micro GC	Vol%	1.4	1.5	1.4	1.6	1.6
Tar content*	SPA	g/Nm^3	13.1	nd	nd	nd	nd

Values are at Normal conditions at temperature of 0 °C (273.15 K) and absolute pressure of 1 atm (1.01325×10^5 Pa).
nd: not determined.
* Higher than toluene, on dry basis.

CH_4 content, compared to that obtained with silica sand, due to its catalytic effect on the reforming of hydrocarbons and tar and the promotion of the water–gas shift (WGS) reaction [30–32]. At position B, downstream OLGA, similar gas composition was obtained.

The average composition of the main gas components at position C (downstream the first AC bed) and E (downstream HDS) was identical to the gas measured at position B (downstream OLGA). The main difference was the H_2 concentration, which was lower at the outlet of the HDS reactor. This is because part of the inlet hydrogen in the gas is consumed by the hydrogenation on unsaturated C=C bonds and hydro-cracking reactions [33]. Additionally, methane concentration is slightly higher at the HDS outlet, due to the hydro-cracking reactions of the saturated hydrocarbons to methane [34,35]. The composition of the main gas compounds at position F (downstream the the ZnO and AC bed), before the bottling station, is similar to position E.

The trace sulphur and hydrocarbon compounds during beech wood gasification, were measured at the sampling positions S1 and S2 by the semi-online μ-GC (every measurement takes approximately 4 min). The data points measured at position A (downstream i-MILENA) are not very reliable as they were monitored before the steady operation. However, once stable the composition is expected to be similar to the one at position B (downstream OLGA). The total concentration of S-species (in the form of H_2S, COS and other S-organic components) was approximately 100 ppmV. This low concentration is attributed to the low content of the corresponding compounds in the original feedstock, shown in Table 1. It is clear that the AC bed (position C) captures the bulk sulphur compounds (H_2S, COS), as their total concentration is reduced to ~2 ppmV. Downstream of the HDS reactor (position E) the H_2S concentration increases slightly due to the hydrodesulfurization of the mercaptans and the hydrolysis of carbonyl sulfide, reactions that produce H_2S [33]. Benzene and toluene are captured by the BTX scrubber to below 100 and 10 ppmV, respectively. The unsaturated hydrocarbons, ethylene and acetylene, are hydrogenated in the HDS reactor to ethane [35] and therefore their concentration is reduced below the detection limit (0.001 vol%), with a simultaneous increase of the ethane concentration.

Prior to gas bottling (position F), all the undesired components (unsaturated hydrocarbons, BTX and Sulphur compounds) were removed to below detection limit levels (10 ppmV) by the last AC and ZnO beds. Benzene concentration was <40 ppmV at the start of the bottling period but it was constantly reduced to around 10 ppmV by the end of the bottling procedure (shown in Figure S6 in the supplementary material).

The total tar concentration – on dry basis – in the raw product gas from beech wood gasification was 13 g/Nm^3. The main tar components formed were polyaromatic (2-ring) components, like naphthalene, along with small concentrations of other light and heavy polyaromatic hydrocarbons (e.g. acenaphtylene, phenanthrene). Aromatic (1-ring) components such as toluene, xylene and styrene, together with heterocyclic aromatic compounds, like cresol and phenol were also detected in smaller concentrations. Downstream of the OLGA reactor, all tar compounds heavier than BTX were almost completely separated from the gas [7].

3.1.2. Lignin

Stable conditions were achieved for about 3 h in the i-MILENA indirect gasifier during lignin gasification. The average temperature in the combustor reactor – above the riser – was around 700 °C, while the average temperature in the BFB gasifier, given by 3 thermocouples located at the bottom, middle and top part of the BFB, was 60 °C higher, around 760 °C. A higher temperature was expected in the riser combustor reactor compared to that of the BFB gasifier, but since the lab-scale system was designed for normal MILENA operation, most of the heat input for gasification temperature control was provided from the external electric trace heating (at the outer part of the BFB reactor). This temperature difference between the gasifier and combustor reactor indicates that less char ends up in the combustor, which is attributed to poor circulation. After 4 h on stream, the temperature in both the riser and the BFB reactor (especially at the bottom) was reduced by 50 °C. Due to the low gasification temperature, a cold zone located on top of the bed plate resulted in lower gas velocity than the critical point for fluidization and thus in poor circulation of char and bed material. To compensate for reduced gas flow in the BFB, nitrogen was added occasionally for a couple of minutes (at 1, 3, 4.8 and 6 h on stream), resulting in a temperature increase back to 760 °C (since more char was introduced in the riser combustor). Additionally, the lignin feeding rate was increased after 4.2 h on steam to 3.5 kg/h, but this was not sufficient as the temperature decreased again at around 5 h on stream. Therefore, the steam rate was increased from 1 to 2.2 kg/h to compensate for reduced gas flow.

The average composition of the gas from lignin gasification – on dry basis – is reported in Table 5. The values of H_2, CO_2 and CH_4, during lignin gasification, downstream i-MILENA and OLGA, were similar to those obtained for beech wood gasification, but the CO concentration appeared significantly lower: 20 vol% compared to 30 vol% for beech wood. The effect of increased steam rate after 5 h on stream was an increase in H_2 concentration, which can be attributed to steam reforming and cracking reactions of the hydrocarbons [6]. In addition, the steam flow increase promotes the water gas shift reaction, resulting in higher H_2 and lower CO concentrations. The H_2/CO ratio was 1.8, which is much higher than that of beech wood gasification.

The gas composition at position C (downstream of the AC bed) was identical to the gas measured at the i-MILENA/OLGA side. At position E (downstream of the HDS), a lower H_2 concentration was observed at the HDS outlet compared to the inlet (position D), similarly to the beech wood gasification. In addition, methane concentration was slightly higher at the HDS outlet due to the hydro-cracking reactions between the saturated hydrocarbons and hydrogen. The main gas composition obtained at position F (downstream of the ZnO and AC bed), before the bottling station, is similar to that of position E.

The composition of sulphur compounds in the gas (H_2S, COS and other S-) during lignin gasification, as measured at positions A and B, was around 10 times higher compared to beech wood gasification. This was expected due to the higher S-content in the original feedstock (see Table 1). The concentration of the C_{2+} hydrocarbons, including toluene, was between 3 and 10 times higher than what was obtained for beech wood, which is attributed both to the lower gasification temperature - that does not promote cracking reactions - and to the multi-ring nature of the lignin molecule. The reduction of the C_2H_4 concentration with time on stream (shown in Figure S10 in supplementary material), measured at positions A and B, is related to the increase of steam rate that promotes cracking reactions of the hydrocarbons, as mentioned earlier.

The AC bed (position C) is able to capture the majority of sulphur compounds. For instance, H_2S concentration is reduced from 1000 ppmV (at position B) to as low as the corresponding value in the beech wood test. Benzene and toluene are captured by the BTX scrubber to around 100 and 10 ppmV, respectively. The unsaturated hydrocarbons, ethylene and acetylene, are hydrogenated in the HDS reactor to ethane, as their concentration is reduced from 3.5 and 0.62, respectively, to below detection limit level, with the simultaneous increase of ethane.

Similarly to beech wood, at position F (downstream the ZnO and AC bed), all the undesired components are removed to below detection limit (10 ppmV) prior to gas bottling.

The total tar concentration – on dry basis – in the product gas from lignin gasification was 21 g/Nm^3, higher than of lignocellulosic biomass due to the multi-ring nature of the lignin molecules, which favors tar formation. The main tar components formed were polyaromatic (2-ring) compounds, like naphthalene, along with small concentrations of other light and heavy polyaromatic hydrocarbons (e.g. acenaphtylene, 2-methylnapthalene, phenanthrene). Heterocyclic aromatic compounds, like phenol, indene and cresol were also detected in significant concentrations. Aromatic (1-ring) components such as toluene, xylene and

Table 5
Gas composition over the sampling positions S1, S2 and S3 during lignin gasification and gas cleaning.

Gas component	Analysis method	Unit	Position A (Downstream MILENA)	Position B (Downstream OLGA)	Position C (Downstream AC)	Position D (Downstream BTX)	Position E (Downstream HDS)	Position F (Downstream AC & ZnO)
Average sampling time (h)			**7–8.5**	**5.5–6**	**7–7.5**	**5–5.5**	**3–4.5**	**6.5–7**
CO	Gas monitor	Vol%	19.8	20.0	20.0	21.0	24.8	23.4
H_2	Gas monitor	Vol%	35.5	34.3	35.8	35.3	26.9	33.3
CO_2	Gas monitor	Vol%	24.4	24.7	24.2	24.5	24.8	24.1
CH_4	Gas monitor	Vol%	11.4	11.7	11.4	11.4	13.3	12.2
N_2	Gas monitor	Vol%	1.4	1.4	1.4	1.6	2.9	2.3
C_2H_2	micro GC	Vol%	0.11	0.12	0.12	0.12	<0.001	<0.001
C_2H_4	micro GC	Vol%	3.3	3.6	3.4	3.5	<0.001	<0.001
C_2H_6	micro GC	Vol%	0.67	0.69	0.67	0.62	4.47	4.43
Benzene	micro GC	ppmV	5972	5576	5897	109	122.5	<10
Toluene	micro GC	ppmV	1911	1609	1848	<10	12.4	<10
Sum C3	GC-FID	ppmV	3622	3113	4426	3290	3207	3380
Sum C4	GC-FID	ppmV	1494	1368	1830	1033	379	10
Sum C5	GC-FID	ppmV	809	736	851	171	31	<1
Sum C6	GC-FID	ppmV	<1	<1	<1	<1	<1	<1
H_2S	S-GC	ppmV	1165	1111	0.9[b]	0.2[c]	8.9	<0.5
COS	S-GC	ppmV	31	55	50	30	0.7	<0.5
Other S-	S-GC	ppmV	50	33	42	1	<0.5	<0.5
Ne tracer gas	micro GC	ppmV	–	812	828	785	1121	768
Ar tracer gas	micro GC	Vol%	2.3	2.4	2.3	2.3	2.9	2.2
Tar content*	SPA	g/Nm^3	21.2	nd	nd	nd	nd	nd

Values are at Normal conditions at temperature of 0 °C (273.15 K) and absolute pressure of 1 atm (1.01325×10^5 Pa).
nd: not determined.
* Higher than toluene, on dry basis.

styrene were formed in small amounts. Again, all tar compounds heavier than BTX were almost completely separated from the gas downstream of the OLGA, [7] as they act as impurity for the fermentation process.

3.2. Syngas fermentation

3.2.1. Beech wood syngas

3.2.1.1. Substrate usage and carbon fixation. The total duration of the fermentation was of 93 h, which is typical for batch fermentations at KIT laboratory, in order to compare between experiments. Several runs with various other gas compositions have shown that around 100 h the culture collapses and yields and productivities start to fall [29]. Table 6 summarizes the main fermentation results from the beech wood test: gas consumption profile, yields, productivity, acetate to ethanol ratio, as well as the percentage of carbon fixed.

The amount of substance flow rate for H_2, CO and CO_2 in the off-gas of the bioreactor for the beech wood syngas fermentation with *C. ljungdahlii* is shown in Fig. 6A. The substrate usage and fixation for this fermentation is depicted in Fig. 7A. The peak observed in the off-gas graph and the sudden decreased in substrate usage or fixation between approximately 39–52 h of process-time were due to an error on the set-up of the pH regulation that led to an increased fermenter volume of up to 1.7 L in all three bioreactors. At 43 h and 67 h the excess fermentation broth was retrieved from the vessels bringing it down to the initial volume of 1.5 L. The amount of products and cell dry weight taken out from the fermenters have been taken into account in the calculations. Nonetheless, the pH was kept constant during this time. The smaller peaks at around 68 h seen in both Fig. 6A and Fig. 7A correspond to the addition of anti-foam to the fermenter, which causes a punctual alteration on the solubility of the gases in the fermenter broth.

During the initial phase of the fermentation (first 5 h), *C. ljungdahlii* mainly used up the fructose carried over from the inoculation culture (data not shown). After this phase, the CO uptake rate by *C. ljungdahlii* increased constantly (Fig. 6A). At 17 h, $\dot{n}_{CO\ out}$ had already decreased to 0.01 mmol/min, which corresponds to the point when the maximum CO

Table 6
Main fermentation results, yield and productivity for the beech wood syngas.

Interval		Unit	Endpoint	Closest to last point of maximum CO fixation	Maximum usage
Process time		h	93	38	17–38
$Y_{P/S,\ used}$		g/g	0.83 ± 0.02	0.85 ± 0.09	0.96 ± 0.12
$Y_{P/S,\ fed}$		g/g	0.33 ± 0.01	0.32 ± 0.03	0.44 ± 0.05
$Y_{P/S,\ fixed}$		g/g	0.97 ± 0.05	0.94 ± 0.13	1.02 ± 0.15
$Y_{P/X}$		g/g	31.9 ± 1.3	14.0 ± 1.7	32.4 ± 5.2
$V_{gas,\ fed}$		L	100.2 ± 0.0	45.8 ± 0.0	25.6 ± 0.0
Acetate:Ethanol		mol/mol	7.8 ± 0.3	16.3 ± 3.4	14.5 ± 1.2
Productivity	Acetate	g/L/h	0.17 ± 0.01	0.17 ± 0.02	0.26 ± 0.06
	Ethanol	g/L/h	0.01 ± 0.00	0.01 ± 0.00	0.01 ± 0.00
	Total	g/L/h	0.18 ± 0.02	0.18 ± 0.02	0.27 ± 0.06
$E_{C,\ total}$		mol %	42.3 ± 0.4	39.7 ± 1.9	55.4 ± 2.3

$Y_{P/S}$ = gram of products (acetate and ethanol) formed per gram of substrate (CO, CO_2 and H_2). This has been calculated per grams of substrate fed, used and fixed. $Y_{P/X}$ = gram of products (acetate and ethanol) per gram of cell dry weight. $P_{product}$ = productivity. Values are given as the average of a triplicate (n = 3) with standard deviations.

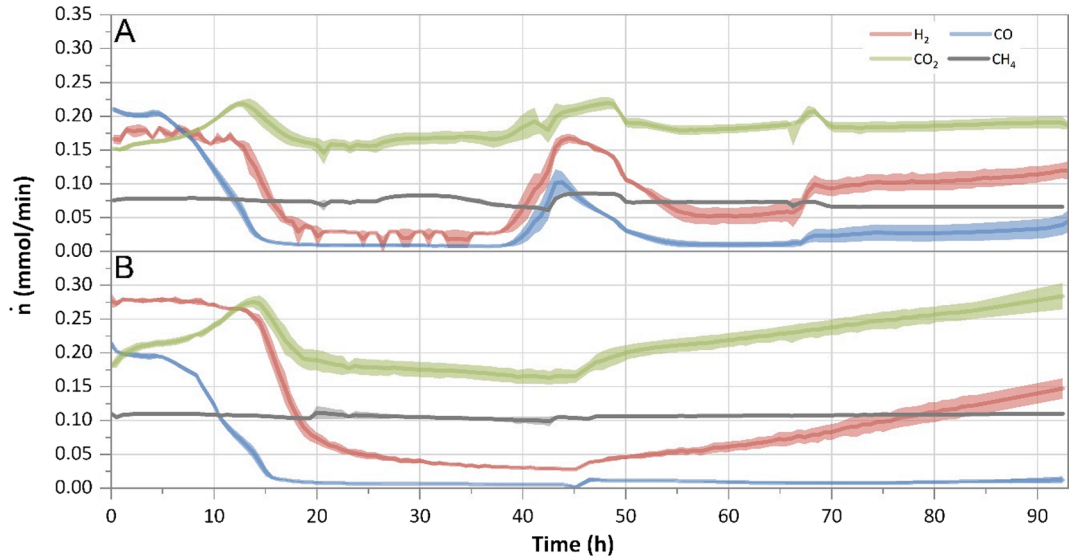

Fig. 6. Amount of substance flow rate in the off-gas for beech wood (A) and lignin (B) syngas fermentation with C. ljungdahlii. Average measured amount of substance flow rate (ṅ) for hydrogen (red), carbon monoxide (blue), carbon dioxide (green) and methane (grey). Lines show the average of a triplicate (n = 3), while the lighter coloured areas depict the standard deviation. A decrease of a substance concentration in the off-gas compared to the starting value indicates its usage. For beech wood (A), the peaks observed between approx. 40 and 55 h are the result of a pH malfunction. (For interpretation of the references to colour in this figure legend, the reader is referred to the web version of this article.)

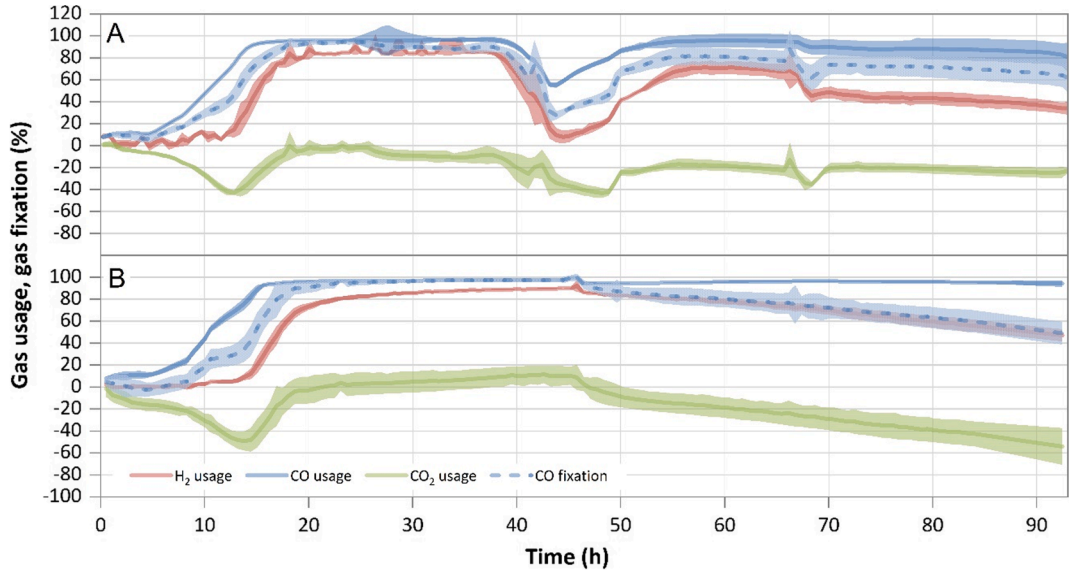

Fig. 7. Substrate usage or fixation for beech wood (A) and lignin (B) syngas. Usage is shown for H_2 (red line), CO_2 (green line) and CO (blue line). CO fixation is depicted by the dotted blue line. The calculated difference between amount of substance flow rate fed into the bioreactor and the amount of substance flow rate detected in the off-gas is shown here as a percentage. Lines show the average of a triplicate (n = 3), while the lighter colored areas depict the standard deviation. A negative substance usage indicates production. For beech wood syngas (A). The peaks observed between approx. 40 and 55 h are the result of a pH malfunction. (For interpretation of the references to colour in this figure legend, the reader is referred to the web version of this article.)

fixation (>85%) started (Fig. 7A). This continued for another 21 h, with an average CO fixation of 91%. Afterwards, due to the interference of the pH regulation issue and the excess broth removal, an increase of CO in the off-gas was observed. After the pH glitch was fixed, CO fixation eventually increased again, reaching an average of 79% from 50 h to 64 h.

Looking at the CO usage (Fig. 7A), it stayed above 85% from 14 h to 40 h, with an average of 95%. The CO usage stayed below that threshold for 10 h, until process-time 50 h, due to the pH regulation glitch. Once it was fixed, it increased again above the 85% mark, staying so up to 90 h, with an average between those times of 91%.

Regarding H_2 uptake, a usage of ≥80% was reached 19 h after inoculation (Fig. 7A). This lasted for at least 20 h (Fig. 7A). Analogously to CO, the effect of the pH regulation malfunction can also be seen in the hydrogen off-gas analysis. The amount of H_2 in the off-gas increased rapidly from 18 h until 45 h of process-time, but after removing excess broth it decreased to a new minimum. The average H_2 usage between 45 h and 61 h was 49%. From this point on, and contrary to what is seen for CO, hydrogen usage did not recover its initial maximum values but rather decreased continuously until the end of the process, with an average of 48%.

As shown in Fig. 7A, CO_2 was produced throughout the fermentation. The initial surge of CO_2, up to approximately 5 h after inoculation, is due to the left-over fructose in the medium. After that, and up to

approximately 12 h, the increase in CO_2 is attributed to the fact that the microorganism was using solely CO, and not H_2, as source of reducing power. As is the case for CO and H_2, the apparent increase in CO_2 production seen at process-time 43 h and 50 h was due to the malfunction of the pH regulation system and the subsequent volume change. Excluding the first 20 h (the initial peak was caused by fructose consumption), CO_2 usage value remained negative, indicating that there was a continuous CO_2 production, ranging from 0.05% to 43%.

The amount of CH_4 detected in the off-gas remained almost constant throughout the fermentation (shown in Fig. 6A). The percentage of total carbon fixed per total carbon fed for the whole process, and up to the maximum CO fixation is shown in Table 6.

3.2.1.2. Cell dry weight, product formation, yield and productivity. The main product formed was acetate, while small concentration of ethanol was also detected, as expected at these conditions [8]. Fig. 8A shows the cell dry weight growth and the products (acetate and ethanol) formation over time. During the first 20 h, the CDW increased rapidly. Afterwards, growth slowed down and reached its maximum measured value of 0.62 g/L at 66.5 h. With respect to product formation, acetate production started immediately after inoculation and the highest rate was observed after 20 h. The final acetate concentration attained was 15.6 g/L. The ethanol concentration in the broth started increasing after 19 h, reaching a value of 1.6 g/L at the end of the process. Apart from acetate and ethanol, no other products could be detected in the fermentation broth. Moreover, the carbon balance could be closed (data not shown), providing proof that all the carbon fixed was in the products and bacterial biomass detected.

Product yields are shown in Table 6 for each of the considered time spans: endpoint, up to the end of maximum CO fixation and during the interval of maximum overall usage. The highest $Y_{P/S}$ values and acetate productivity were obtained during the maximum overall usage interval, while ethanol productivity was stable for the three intervals.

3.2.2. Lignin syngas

3.2.2.1. Substrate usage and carbon fixation. The total process time for the lignin fermentation experiment was also 93 h, as in the beech wood test. Table 7 summarizes the main fermentation results from the lignin test: gas consumption profile, yields, productivity, acetate to ethanol ratio, as well as the percentage of carbon fixed, for the three different, relevant time frames.

For the lignin fermentation, the amount of substance flow rate for H_2, CO and CO_2 detected in the bioreactor off-gas is shown in Fig. 6B, and the substrate usage and fixation for this fermentation are illustrated in Fig. 7B. In both Fig. 6B and Fig. 7B, a small disturbance in the gas leaving the bioreactor can be seen around 45 h, which was caused by the addition of antifoam.

As in the BWS fermentation, during the initial phase (first 5 h), the microorganism used up an average of 0.54 g/L of fructose that were left

Table 7
Main fermentation results, yield and productivity for the lignin syngas.

Interval		Unit	Endpoint	Closest to last point of maximum CO fixation	Maximum usage
Process time		h	93	52	22–48
$Y_{P/S,\ used}$		g/g	0.79 ± 0.02	0.89 ± 0.02	0.84 ± 0.07
$Y_{P/S,\ fed}$		g/g	0.30 ± 0.01	0.32 ± 0.00	0.40 ± 0.02
$Y_{P/S,\ fixed}$		g/g	0.92 ± 0.07	0.94 ± 0.06	0.84 ± 0.07
$Y_{P/X}$		g/g	31.8 ± 2.3	18. 9 ± 0.7	33.4 ± 2.8
$V_{gas,\ fed}$		L	127.7 ± 0.0	68.3 ± 0.0	35.2 ± 0.0
Acetate:Ethanol		mol/mol	5.2 ± 0.5	17.4 ± 2.8	16.2 ± 1.9
Productivity	**Acetate**	g/L/h	0.16 ± 0.01	0.19 ± 0.00	0.23 ± 0.01
	Ethanol	g/L/h	0.02 ± 0.00	0.01 ± 0.00	0.01 ± 0.00
	Total	g/L/h	0.18 ± 0.01	0.20 ± 0.00	0.24 ± 0.01
$E_{C,\ total}$		mol %	42.1 ± 4.1	45.4 ± 5.9	55.9 ± 3.6

$Y_{P/S}$ = gram of products (acetate and ethanol) formed per gram of substrate (CO, CO_2 and H_2). This has been calculated per grams of substrate fed, used and fixed. $Y_{P/X}$ = gram of products (acetate and ethanol) per gram of cell dry weight. $P_{product}$ = productivity. Values are given as the average of a triplicate (n = 3) with standard deviations.

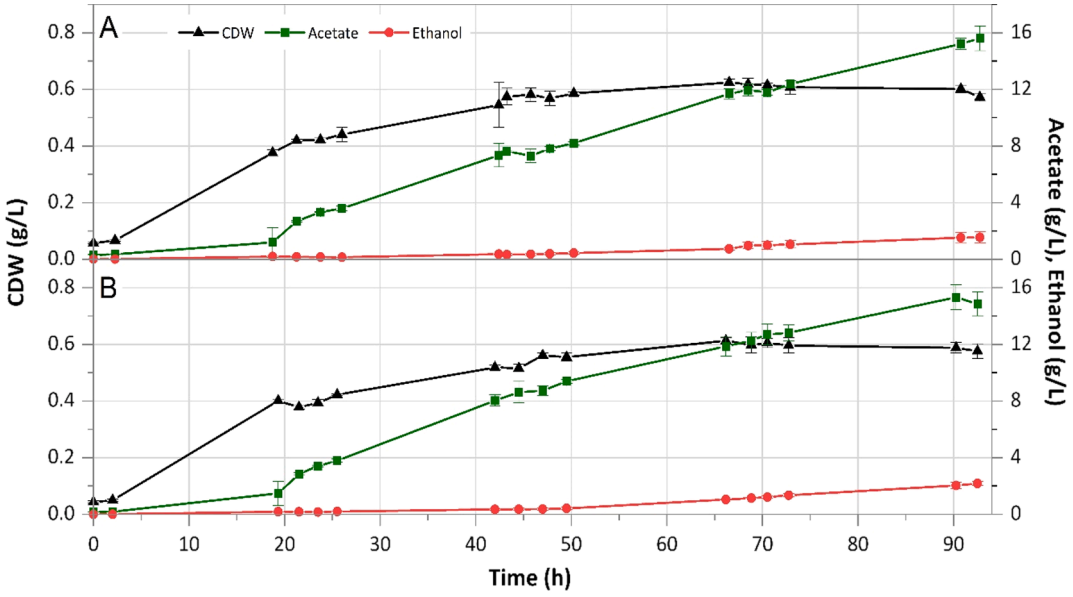

Fig. 8. Growth and product formation profiles for beech wood (A) and lignin (B) syngas. Points indicate actual samples. Lines are only depicted for clarity purposes; error bars show the standard deviation among the triplicate. CDW = cell dry weight.

as a carry-over from the inoculation culture (data not shown). CO uptake started directly afterwards. Both fermentations showed a comparable trend, with similar values for $\dot{n}_{CO,\ out}$ at similar times. Hence, the different syngas source and composition did not have an impact on the performance of the cells during this first phase. At 18 h, CO fixation reached 87%. This is the starting point for the maximum CO fixation interval, which continued for 34 h. The average CO fixation calculated for this time period is 95%. From 52 h of process-time up to the end of the fermentation the average for the percentage of carbon fixed was 73%. The average from 64 h to the end of the process was 68%.

The microorganism performed consistently in both experiments, regarding CO fixation: firstly, the time required to reach 85% CO fixation is equivalent in both cases: 17 h for BWS and 18 h for LS. Despite not being able to compare the period during which the pH glitch happened, after that, between 51 h (BWS) or 52 (LS) h and 64 h the average was 79% and 81% respectively. Finally, the behavior of *C. ljungdahlii* from 52 h to the end of the process was also almost identical in both cases.

CO usage reached 89% after 15 h and was maintained from that point throughout the duration of the process, at an average value of 96%, as opposed to what is seen with BWS, where a decrease is detected towards the end.

Concerning H_2, the threshold of 80% usage was achieved at 23 h and lasted for 34 h, as shown in Fig. 7B. From that point, the amount of H_2 in the off-gas steadily increased. The average usage between 57 h and the end sample was 68%. Comparing the gas usage for both fermentations, it is observed that the graphs look similar (excluding the pH issue), having a first phase where H_2 is consumed at around 80%, and then decreasing towards the end. It is interesting to notice that the flow rate of H_2 or the H_2:C_{total} ratio does not appear to have an effect on the gas usage, since even if it was lower in the BWS than in the LS, both fermentations performed similarly.

As opposed to what is seen in the BWS fermentation, where no CO_2 usage was seen, in the LS fermentation CO_2 was used between process-time 22 h and 46 h, with an average of 6%. The maximum CO_2 usage achieved was 12% at 42.6 h. The variation in the range of values after 20 h was wider, compared to that of BWS: from 11.7% to −54%.

As seen in the BWS fermentation, CH_4 did not appear to have any effect in the process, since the microorganisms lack the ability to use it. It also did not produce any noticeable effect in growth or product formation, and can be considered, in this case, inert. This result is in line with what has been reported in the literature [36].

Regarding the other compounds present in both BWS and LS, such as C_2H_6, Ahmed et al. [13] did not notice any influence in the fermentation performance. On the other hand, unsaturated hydrocarbons, such as C_2H_4, have been described as an inhibitor for methanogenic bacteria which inhibits the hydrogenases [37,38]. At the concentration present in both BWS and LS after cleaning (<0.001 ppm) it can be said it did not cause any detrimental effect.

The percentage of total carbon that *C. ljungdahlii* was able to fix per carbon fed ($E_{C,total}$) during the entire LS fermentation is shown in Table 7. This parameter enables the comparison of the performance between different experiments, as well as serving as an indication of the fitness level of the cells at different stages of the fermentation. It is noticeable that not all carbon fed into the bioreactor could be captured, but in both cases the calculated endpoint values are very similar (Table 6 and Table 7). Therefore, the slightly different gas composition obtained from the gasification of beech wood and lignin and the presence of unidentified trace impurities, did not influence the fermentation outcome in terms of affecting the ability of *C. ljungdahlii* to fix the carbon fed.

3.2.2.2. Cell dry weight, product formation, yield and productivity. Fig. 8B shows the cell dry weight growth and the products (acetate and ethanol) formation over time for the LS fermentation. The maximum CDW achieved was 0.61 g/L (at 66 h) before the growth stopped. At the process ending point, the value measured was 0.6 g/L (Fig. 8B). Both BWS and LS fermentations showed an almost identical profile regarding bacterial biomass production.

Acetate formation could be detected already with the first samples, however the highest production rate was achieved after around 20 h, as in the beech wood syngas fermentation test. The final measured acetate concentration in the fermentation medium of 14.9 g/L, slightly lower than the BWS test. The ethanol concentration in the fermenter was 0.2 g/L after 19 h, and reached a maximum of 2.2 g/L at the end of the process, slightly higher than for BWS. As for BWS, no other products were detected in this fermentation, and the carbon balance could also be closed.

As shown in Table 7, also in this case the highest $Y_{P/S\ used}$ and $Y_{P/S\ fixed}$ obtained during the maximum overall usage period. Acetate productivity also reached its maximum during the same period, while ethanol productivity was highest when calculated up to the end of the process. This is caused by the ethanol production starting towards the end of the process, after growth slows down, which is a well-documented behavior in *C. ljungdahlii* [39]. For the LS, the product profile at the endpoint was shifted towards ethanol. The other two intervals, on the contrary, presented a slightly higher ratio compared to beech wood.

End-point yields and productivities achieved are comparable for both BWS and LS. The most noticeable difference is found during the maximum usage interval, where BWS performed better than LS. Regarding product ratios, the LS fermentation presented a higher molar ethanol to acetate ratio at the endpoint, although it was the opposite at the other two intervals considered, suggesting that a metabolic shift happened towards the end of the fermentation.

3.2.3. Syngas fermentation results overview

Despite the different thermochemical properties of lignin compared to beech wood, the operational conditions applied during indirect gasification in i-MILENA resulted in a similar gas composition regarding the main gas components. Furthermore, the gas cleaning steps applied downstream were able to reduce the impurities that could impose danger to the microorganism of the fermentation process, such as H_2S, COS, unsaturated hydrocarbons and aromatic compounds, resulting in similar gas qualities for both feedstocks. Datar et al. [36] studied the fermentation of switch grass derived syngas by *Clostridium carboxidivorans* P7. They reported that the impurities present in the syngas after partial cleaning (4.2% CH_4, 2.4% C_2H_4 and 0.8% C_2H_6, as well as small concentrations of nitric oxide and acetylene) had a great impact, inhibiting bacterial biomass growth and H_2 usage. This could be attributed mainly to the unsaturated hydrocarbons left in the syngas, as in the work presented here, the main gas compound left in the syngas, apart from H_2/CO/CO_2, was CH_4 (approximately 12 vol%) but no inhibition of growth or gas consumption was observed.

Moreover, in a calculation based on the commercial LanzaTech process, the carbon conversion efficiency results in 51.6% [10]. In this study, values around 55% for carbon fixation onto products are achieved for both BWS and LS during maximum usage interval, showing that this system has potential to be further developed. 99% of the carbon fixed could be detected in the products and bacterial biomass, with the remaining used carbon being accounted for as produced CO_2. The performance of this process is comparable to another one reported in literature, [13] where 97% of the utilized carbon was detected in the bacterial biomass, the product and the produced CO_2.

The production of CO_2 for both BWS and LS cases is expected due to the stoichiometry of the acetogenic Wood-Ljungdahl-Pathway: if not enough H_2 is present, or if its usage stops as seen here, CO is used as the only energy source and CO_2 is inevitably formed [40]. One solution to avoid CO_2 release in the atmosphere, is the recirculation of the off-gas in combination with addition of extra H_2 (potentially generated from excess electricity or other renewable sources) in the appropriate stoichiometric ratio. In any case, the CO_2 produced in this system is green

since it originates from lignin or beech wood gasification and its environmental impact is limited. Alternative, it could be captured from the off-gas similarly to a chemical catalytic system (e.g. using an amine scrubber), resulting in negative CO_2 emissions.

Methane seems to have an insignificant effect on the bacteria, acting as an inert for the fermentation. This is crucial for the integration of the two processes, since it is present in the syngas at approximately 12 vol%, for both BWS and LS, and its removal prior to the fermentation would result in increased costs. The methane left in the off-gas can be easily valorized as a source of energy improving the overall efficiency.

The behavior of the microorganism used in this batch fermentation system, in terms of gas usage and fixation, is in accordance with others published studies [8,41]. In all cases, a first phase can be observed where CO starts to be consumed, together with the production of CO_2. H_2 consumption starts after the dissolved CO amount in the broth decreases, and the production of CO_2 lowers. Following this, a stage where total CO and H_2 consumption is observed, with varying duration depending on the gas composition and process parameters, and finally, the culture stops growing and gas consumption starts to decrease. Thus, it can be concluded that no significant change in behavior was observed in the culture due to the presence of impurities.

Ethanol is a more valuable compound than acetate, and an increase in the ethanol to acetate ratio is an interesting effect of biomass-derived syngas when compared to model syngas [41]. Optimization of the process, like selecting a strain for higher ethanol titers and establishing a continuous or a two-stage system, as has already been demonstrated by Richter et al. [42] could make the overall process more economically attractive.

A previously reported fermentation with a synthetic mixed, model syngas was performed in the same system and under the same conditions. The gas contained only CO, CO_2 and H_2 (32.5% CO, 16.0% CO_2 and 32.5 %H_2, with a flow rate of 18.0 L/min) [29]. Compared to the synthetic-mixed syngas where no other unidentified trace compounds were present, the same value for the ethanol/acetate ratio was obtained for the BWS, but an increased ethanol production could be seen towards the end in LS, similarly to other studies [13,36]. The reason why ethanol production did not increase in BWS compared to the synthetic-mixed syngas remains to be investigated. A potential reason could be the difference in the gas composition, known to affect the fermentation outcome, [43] or due to the present of some unidentified trace gas components. Most studies found in literature are focused on the effects of the ratio of only two of the syngas components (CO/CO_2, H_2/CO_2, CO/H_2), without any impurity present. The combined synergistic effects of different $CO/CO_2/H_2$ blends, together with impurities, has not been widely considered. Valgepea et al. found that more ethanol was produced by *Clostridium autoethanogenum* when grown on H_2/CO compared to when grown on pure CO, [44] but in the case here presented, the higher H_2/CO ratio of the BWS did not cause this effect. This highlights the need for more research efforts towards linking the gasification and fermentation technologies, and the limitation of extrapolating results from clean gas mixtures to biomass-derived syngas. Hurst and Lewis [43] reported that, when growing *Clostridium carboxidivorans P7* in CO/CO_2 gas mixtures, an increase of the CO partial pressure resulted in increased ethanol production. Higher CO concentrations also directed *Clostridium ljungdahlii* product formation towards ethanol when grown with H_2/CO [45]. Hence, the higher amount of CO present in the LS could be a reason for the higher ethanol production, compared to BWS.

Comparison of the carbon conversion efficiencies, $E_{C,total}$, between the synthetic-mixed syngas and those of the BWS and LS, showed that the clean syngas provided a higher carbon fixation ratio in all cases, achieving between 4 and 10% higher carbon fixation [29]. This difference could be attributed to the presence of some trace impurities left in the syngas (e.g. C3 + hydrocarbons, <10 ppm BTX) or other unidentified trace compounds (e.g. HCN). However, as mentioned previously, the gas composition was also slightly different, and it can have significant impact on the fermentation outcome [36,46]. Regarding productivities, at the endpoint it was 22% higher (0.22 g/L/h) than the BWS and LS fermentations (Table 6 and Table 7); up to the point of maximum CO fixation, it was 46% and 34% higher (0.27 g/L/h) than BWS and LS, respectively. During maximum overall usage the difference decreased, with the synthetic-mixed syngas being only 8% (0.26 g/L/h) above both BWS and LS. The yields achieved per substrate fed ($Y_{P/S,fed}$) at the endpoint by both the BWS and LS were also slightly lower: the synthetic-mixed syngas reached a value of 0.43 g/g, 23% and 30% higher than BWS and LS, respectively. Despite the negative impact of impurities in the syngas that has been documented broadly in literature [14,16,47], the cleaning process applied in this case has been proven sufficient, as the endpoint yield per carbon fixed ($Y_{P/S,\ fixed}$) did not change significantly and remained mainly unaltered in both cases when compared to the impurity-free syngas.

4. Conclusions

This work demonstrates the combination indirect gasification with the syngas fermentation for the production of bulk chemicals and biofuels. The aim is to provide an insight of the indirect gasification of lignin, the gas cleaning applied to reduce unwanted compounds of the product gas, study the effect of the main impurities left in the gas and the outcomes of lignin derived syngas fermentation.

Very few studies have been published where biomass-derived syngas is used as fermentation substrate, and even fewer report the linking of the gasification and fermentation technology. Gas contaminants like tar compounds, acetylene, ethylene and benzene, have been found to reduce the fermentability of the gas when using acetogenic organisms. However, the effect of methane, higher hydrocarbons and sulphur compounds is not clear.

The product gas derived from lignin indirect gasification contains, apart from H_2, CO and CO_2, also CH_4 (up to 12 vol%), C2 + hydrocarbons, BTX, tar and sulphur compounds. After the cleaning process applied at TNO, the main impurities identified in the lignin syngas are CH_4 and saturated C2-C4 hydrocarbons. Similar content of impurities was realized for the beech wood syngas after the same cleaning steps. The results presented here show the successful integration lignin gasification and fermentation. The gas cleaning process applied for both beech wood and lignin feedstocks was found sufficient for using the gas as fermentation substrate by *C. ljungdahlii*, since no cell dormancy, or substrate consumption inhibition could be observed. Furthermore, the fermentation results are comparable for both gases.

As a next step, it is interesting to study the effect of some impurities, such as the unsaturated hydrocarbons and the S-compounds, on the fermentation process by *Clostridium ljungdahlii*. This would result in a simpler gas cleaning process, thus reducing the cost. Additionally, the fermentation of biomass-derived syngas in a continuous process would be of use in order to assess productivities and yields over a longer term, with cells being exposed to impurities for a prolonged period of time.

Further optimization studies are necessary to achieve a better carbon fixation capacity, as well as to boost productivities, in order to improve the economic feasibility of the overall process. The co-production of bio-BTX may successfully fulfill the requirements for green production of organic or aromatic intermediates for the chemical industry in the near future. Additionally, the off-gas of the fermentation process that contains significant amount of methane, ethane and traces of higher hydrocarbons, can be utilized in other applications, thus improving the efficiency and the economic benefits of the integrated process.

CRediT authorship contribution statement

E.T. Liakakou: Conceptualization, Investigation, Writing - original draft, Writing - review & editing. **A. Infantes:** Conceptualization, Writing - original draft, Writing - review & editing. **A. Neumann:** Conceptualization, Supervision. **B.J. Vreugdenhil:** Conceptualization, Supervision, Writing - review & editing, Resources, Project

administration, Funding acquisition.

Declaration of Competing Interest

The authors declare that they have no known competing financial interests or personal relationships that could have appeared to influence the work reported in this paper.

Acknowledgement

This work has received finding from the European Union's Horizon 2020 research and innovation programme under grant agreement No. 731263.

Appendix A. Supplementary data

Supplementary data to this article can be found online at https://doi.org/10.1016/j.fuel.2020.120054.

References

[1] Ambition research official website: https://www.ambition-research.eu/ [Accessed on 10-2-2020].
[2] Pandey MP, Kim CS. Lignin depolymerization and conversion: a review of thermochemical methods. Chem Eng Technol 2011;34(1):29–41.
[3] Cerone N, Zimbardi F, Contuzzi L, Prestipino M, Carnevale MO, Valerio V. Air-steam and oxy-steam gasification of hydrolytic residues from biorefinery. Fuel Process Technol 2017;167:451–61. https://doi.org/10.1016/j.fuproc.2017.07.027.
[4] Cerone N, Zimbardi F, Contuzzi L, Alvino E, Carnevale MO, Valerio V. Updraft gasification at pilot scale of hydrolytic lignin residue. Energy Fuel 2014;28:3948–56. https://doi.org/10.1016/j.fuproc.2017.07.027.
[5] Pinto F, André RN, Carolino C, Miranda M, Abelha P, Direito D, Dohrup J, Sørensen HR, Girio F. Effects of experimental conditions and of addition of natural minerals on syngas production from lignin by oxy-gasification: comparison of bench- and pilot scale gasification. Fuel 2015;140:62–72. https://doi.org/10.1016/j.fuel.2014.09.045.
[6] Liakakou ET, Vreugdenhil BJ, Cerone N, Zimbardi F, Pinto F, André R, et al. Fuel 2019;251:580–92. https://doi.org/10.1016/j.fuel.2019.04.081.
[7] Kuo Y-T, Almansa GA, Vreugdenhil BJ. Catalytic aromatization of ethylene in syngas from biomass to enhance economic sustainability of gas production. Appl Energy 2018;215:21–30. https://doi.org/10.1016/j.apenergy.2018.01.082.
[8] Oswald F, Dörsam S, Veith N, Zwick M, Neumann A, Ochsenreither K, et al. Sequential Mixed Cultures: From Syngas to Malic Acid. Front Microbiol 2016;7(891):1–12. https://doi.org/10.3389/fmicb.2016.00891.
[9] Liew FM, Martin ME, Tappel RC, Heijstra BD, Mihalcea C, Köpke M. Gas Fermentation – A Flexible Platform for Commercial Scale Production of Low Carbon Fuels and Chemicals from Waste and Renewable Feedstocks. Front Microbiol 2016;7(694):1–28. https://doi.org/10.3389/fmicb.2016.00694.
[10] Griffin DW, Schultz MA. Fuel and Chemical Products from Biomass Syngas: A Comparison of Gas Fermentation to Thermochemical Conversion Routes. Environ Prog Sustain Energy 2012;31:219–24. https://doi.org/10.1002/ep.
[11] Daniell J, Köpke M, Simpson SD. Commercial Biomass Syngas Fermentation. Energies 2012;5,5372–417. doi: 10.3390/en5125372.
[12] Cao Z, Hu T, Guo J, Xie J, Zhang N, Zheng J, Che L, Chen BH. Stable and facile ethanol synthesis from syngas in one reactor by tandem combination CuZnAl-HZSM-5, modified-H-Mordenite with CuZnAl catalyst. Fuel 2019;254:115542. https://doi.org/10.1016/j.fuel.2019.05.125.
[13] Ahmed A, Cateni BG, Huhnke RL, Lewis RS. Effects of biomass-generated producer gas constituents on cell growth, product distribution and hydrogenase activity of *Clostridium carboxidivorans* P7T. Biomass Bioenergy 2006;30(7):665–72. https://doi.org/10.1016/j.biombioe.2006.01.007.
[14] Xu D, Tree DR, Lewis RS. The effects of syngas impurities on syngas fermentation to liquid fuels. Biomass Bioenergy 2011;35(7):2690–6. https://doi.org/10.1016/j.biombioe.2011.03.005.
[15] Chiche D, Diverchy C, Lucquin A-C, Porcheron F, Defoort F. Synthesis Gas Purification. Oil Gas Sci Technol – Rev IFP Energies nouvelles 2013;68(4):707–23. https://doi.org/10.2516/ogst/2013175.
[16] Ramachandriya KD, Kundiyana DK, Sharma AM, Kumar A, Atiyeh HK, Huhnke RL, et al. Critical factors affecting the integration of biomass gasification and syngas fermentation technology. AIMS Bioeng 2016;3:188–210. https://doi.org/10.3934/bioeng.2016.2.188.
[17] 09/08, N. p. Review of Technologies for Gasification of Biomass and Wastes, UK: E4tech, NNFCC; 2009.
[18] Taherzadeh MJ, Chandolias K, Richards TE. Combined gasification-fermentation process in waste biorefinery, in Waste Biorefinery: Potential and Perspectives, 157-200. Elsevier Ltd.; 2018, doi: 10.1016/B978-0-444-63992-9.00005-7.
[19] Mock J, Zheng Y, Mueller AP, Ly S, Tran L, Segovia S, Nagaraju S, Köpke M, Dürre P, Thauer RK, Metcalf WW. Energy Conservation Associated with Ethanol Formation from H 2 and CO 2 in Clostridium autoethanogenum Involving Electron Bifurcation. J Bacteriol 2015;197(18):2965–80. https://doi.org/10.1128/JB.00399-15.
[20] Heijstra BD, Leang C, Juminaga A. Gas fermentation: cellular engineering possibilities and scale up. Microb Cell Fact 2017;16(1). https://doi.org/10.1186/s12934-017-0676-y.
[21] Teixeira LV, Moutinho LF, Romao-Dumaresq AS (201). Gas fermentation of C1 feedstocks.s.
[22] Lane J. On the mend: Why INEOS Bio isn't producing ethanol in Florida. Biofuels Dig; 2014. http://www.biofuelsdigest.com/bdigest/2014/09/05/on-the-mend-why-ineos-bio-isnt-reporting-much-ethanol-production/ [Accessed on 13-5-20].
[23] Karlson B, Bellavitis C, France N, Manage J. Commercializing LanzaTech, from waste to fuel: An effectuation case. J Manag Organ 2018;1–22. https://doi.org/10.1017/jmo.2017.83.
[24] Sekisui chemical co., ltd. Turning "Garbage" into Ethanol: https://www.sekisuichemical.com/whatsnew/2017/1325318_29675.html [Accessed on 20-5-2020].
[25] Widjaya ER, Chen G, Bowtell L, Hills C. Gasification of non-woody biomass: A literature review. Renew Sustain Energy Rev 2018;89:184–93. https://doi.org/10.1016/j.rser.2018.03.023.
[26] Fryda LE, Panopoulos KD, Kakaras E. Agglomeration in fluidised bed gasification of biomass. Powder Technol 2008;181(3):307–20. https://doi.org/10.1016/j.powtec.2007.05.022.
[27] Phyllis 2. ECN database for biomass and waste: https://phyllis.nl/ [Accessed on 10-11-2020].
[28] van der Meijden CM. Development of the MILENA gasification technology for the production of BioSNG, Eindhoven: Technische Universiteit Eindhoven; 2010, doi: 10.6100/IR691187.
[29] Infantes A, Kugel M, Neumann A. Evaluation of Media Components and Process Parameters in a Sensitive and Robust Fed-Batch Syngas Fermentation System with Clostridium ljungdahlii. Fermentation; 2020. doi: 10.3390/fermentation6020061.
[30] Virginie M, Adánez J, Courson C, de Diego LF, García-Labiano F, Niznansky D, Kiennemann A, Gayán P, Abad A. Effect of Fe–olivine on the tar content during biomass gasification in a dual fluidized bed. Appl Catal B 2012;121-122:214–22.
[31] Devi L. Catalytic removal of biomass tars, Olivine as prospective in-bed catalyst for fluidized-bed biomass gasifiers, Doctoral Thesis, Eindhoven University of Technology; 2005, ISBN: 90-386-2906-0.
[32] Aranda G, van der Drift A, Vreugdenhil BJ, Visser HJM, Vilela CF, van der Meijden CM; 2014.
[33] Sánchez-Delgado RA. Hydrodesulfurization and Hydrodenitrogenation, in D. Michael P. Mingos and R.H. Crabtree (Eds), Comprehensive Organometallic Chemistry III, From Fundamentals to Applications. Elsevier Ltd.; 2007, p. 759–800, doi: 10.1016/B0-08-045047-4/00029-7.
[34] Horáček J, Kubička D. Bio-oil hydrotreating over conventional CoMo & NiMo catalysts: The role of reaction conditions and additives. Fuel 2017;198:49–57. https://doi.org/10.1016/j.fuel.2016.10.003.
[35] Wang H, Li G, Rogers K, Lin H, Zheng Y, Ng S. Hydrotreating of waste cooking oil over supported CoMoS catalyst – Catalyst deactivation mechanism study. Molecular Catalysis 2017;443:228–40. https://doi.org/10.1016/j.mcat.2017.10.016.
[36] Datar RP, Shenkman RM, Cateni BG, Huhnke RL, Lewis RS. Fermentation of biomass-generated producer gas to ethanol. Biotechnol Bioeng 2004;86(5):587–94. https://doi.org/10.1002/bit.20071.
[37] Sprott GD, Jarrell KF, Shaw KM, Knowles R. Acetylene as an Inhibitor of Methanogenic Bacteria. Microbiology 1982;128(10):2453–62. https://doi.org/10.1099/00221287-128-10-2453.
[38] Zorin NA, Dimon B, Gagnon J, Gaillard J, Carrier P, Vignais PM. Inhibition by Iodoacetamide and Acetylene of the H-D-Exchange Reaction Catalyzed by *Thiocapsa Roseopersicina* Hydrogenase. Eur J Biochem 1996;241(2):675–81. https://doi.org/10.1111/j.1432-1033.1996.00675.x.
[39] Richter H, Molitor B, Wei H, Chen W, Aristilde L, Angenent LT. Ethanol production in syngas-fermenting *Clostridium ljungdahlii* is controlled by thermodynamics rather than by enzyme expression. Energy Environ Sci 2016;9(7):2392–9. https://doi.org/10.1039/C6EE01108J.
[40] Phillips JR, Huhnke RL, Atiyeh HK. Syngas Fermentation: A Microbial Conversion Process of Gaseous Substrates to Various Products. Fermentation 2017;3:28. https://doi.org/10.3390/fermentation3020028.
[41] Infantes A, Kugel M, Raffelt K, Neumann A. Side-by-side comparison of clean and biomass- 3 derived, impurity-containing syngas as substrate for 4 acetogenic fermentation with *Clostridium ljungdahlii*. Fermentation 2020;6(3):84. https://doi.org/10.3390/fermentation6030084.
[42] Richter H, Martin ME, Angenent LT. A Two-Stage Continuous Fermentation System for Conversion of Syngas into Ethanol. Energies 2013;6(8):3987–4000. https://doi.org/10.3390/en6083987.
[43] Hurst KM, Lewis RS. Carbon monoxide partial pressure effects on the metabolic process of syngas fermentation. Biochem Eng J 2010;48(2):159–65. https://doi.org/10.1016/j.bej.2009.09.004.
[44] Valgepea K, de Souza Pinto Lemgruber R, Abdalla T, Binos S, Takemori N, Takemori A, Tanaka Y, Tappel R, Köpke M, Simpson SD, Nielsen LK, Marcellin E. H_2 drives metabolic rearrangements in gas-fermenting *Clostridium autoethanogenum*. Biotechnol Biofuels 2018;11(1). https://doi.org/10.1186/s13068-018-1052-9.

[45] Jack J, Lo J, Maness P-C, Ren ZJ. Directing *Clostridium ljungdahlii* fermentation products via hydrogen to carbon monoxide ratio in syngas. Biomass Bioenergy 2019;124:95–101. https://doi.org/10.1016/j.biombioe.2019.03.011.

[46] Bengelsdorf FR, Straub M, Dürre P. Bacterial synthesis gas (syngas) fermentation. Environ Technol 2013;34(13-14):1639–51. https://doi.org/10.1080/09593330.2013.827747.

[47] Munasinghe PC, Khanal SK. Biomass-derived syngas fermentation into biofuels: Opportunities and challenges. Biofuels 2011;101:79–98. https://doi.org/10.1016/B978-0-12-385099-7.00004-8.